Progress In Electromagnetics Research, Vol. 135, 281–296, 2013

SIMPLIFICATION METHOD FOR MODELING CROSSTALK OF MULTICOAXIAL CABLE BUNDLES

Liangliang Liu[1], Zhuo Li[1, 2, *], Jian Yan[1], and Changqing Gu[1]

[1]College of Electronic and Information Engineering, Nanjing University of Aeronautics and Astronautics, Nanjing 210016, China

[2]State Key Laboratory of Millimeter Waves, Southeast University, Nanjing 210096, China

Abstract—In this work, a new efficient simplification method is proposed for crosstalk prediction of multicoaxial cable bundles (MCCB). The purpose of the new simplification method is to reduce the simulation time by reducing the complexity of the complete cable bundle model. A modified five-step procedure is established to define the electrical and geometrical characteristics of the reduced cable bundle by making the outer and inner conductor of the coaxial cable participate in the equivalence procedure respectively. After a short presentation of the MCCB coupling problem, the theory fundamentals of the new simplification method and numerical simulations performed on a simple MCCB are presented to demonstrate the efficiency and the advantages of the new simplification method.

1. INTRODUCTION

In high data rate and high security systems, signal transmissions are often performed on shielded cables or coaxial cables (CCs). And also in modern avionic control systems, many control signals for adjusting the flight attitude through rotating the flap are transmitted through CCs. The CCs in such systems are often grouped together with other high intensity power lines into closely coupled cable bundles due to limited installation space. Crosstalk can take place and threaten the flight safety. So it is imperative to study the crosstalk mechanism that could happens. The coaxial cable can be divided into two transmission line systems; one is the inner conductor (IC) system, and the other

Received 14 November 2012, Accepted 18 December 2012, Scheduled 24 December 2012
* Corresponding author: Zhuo Li (lizhuo@nuaa.edu.cn).

is the external shield system [1]. Electromagnetic (EM) interference produced by external interference sources can propagate along the shield, and if the shield is not perfectly grounded and the EM field will penetrate the shield, and cause some unnecessary interference responses along the internal conductor and neighboring cables. The degree of coupling depends on the internal and external loading conditions, shield structure, and spacing between the cables and the presence of any other conducting materials [2]. Thus, determination of the terminal crosstalk [3–5] response of these cable bundles is becoming increasingly important.

Parallel coaxial cable bundle can be considered as uniform multiconductor transmission line network (MTLN) system. There are several articles focusing on the applications of different nonuniform transmission lines for power divider design [6–8] and impedance measurements [9]. The coupling between two CCs was directly solved by transmission line equations [1]. For more than two cables, however, the coupling model is complicated by the mutual couplings between the receptor circuits. Other efficient numerical techniques exist for crosstalk prediction of multicoaxial cable bundle (MCCB) systems [2] by using the transfer impedance [10], modal decomposition [11] and eigenvalue method [12]. However, these methods all have the disadvantage of high memory requirements and long simulation time.

In recent years, an effective numerical modeling technique called the "Equivalent Cable Bundle Method" (ECBM) based on a main assumption that the common-mode response is more critical than the differential-mode response proposed in the model reduction and prediction of EM immunity [13], emissions [14] and crosstalk [15] of complex cable bundles over a large frequency range. Although the ECBM can give satisfactory results for cable bundles composed of single wire cables or twisted pair cables [16], little attention has been paid to the model simplification of the MCCB. So, in this work, we

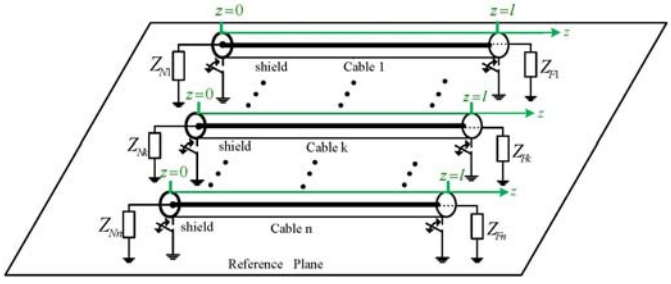

Figure 1. Illustration of A MCCB model.

will focus on the EM crosstalk prediction of the MCCB as shown in Figure 1, and a new efficient simplification method is proposed, which is based on a modified five-step procedure to define the electrical and geometrical characteristics of the reduced cable bundle (RCB) by making the shield and the IC of the CCs participate in the equivalence procedure, respectively.

The organization of this paper is as follows. In Section 2, the theory fundamentals and a modified five-step equivalent process are presented. In Section 3, simulation results are given on EM crosstalk prediction to validate the proposed method, and Section 4 draws some concluding remarks.

2. PRESENTATION OF THE SIMPLIFICATION METHOD

In this section, after some presentation of general conditions of the new simplification method, a modified five-step procedure will be established to define the electrical and geometrical characteristic parameters of the RCB in the following paragraphs.

2.1. General Conditions

For the coupling problem of the MCCB, solid cylindrical shields consisting of perfect electric conductor (PEC) provide complete isolation theoretically, but for braided shields there exists coupling to the interior wire via the holes in the braid. Also, imperfect conductor shields provide for an additional coupling mechanism via diffusion through the shield wall [1]. In this paper only braided CCs are considered.

A braided coaxial cable consists of an IC surrounded by a circular shield composed of strands of wires interwoven helically around a common axis to provide flexibility [2]. If the shield is connected to the ground plane at either end and electrically short, the shield voltage will be essentially zero at all points along the shield so that the electric field coupling to the receptor wire from the generator wire is eliminated [1]. If the shield is connected to the ground plane at both ends, a current will generate a counteracting magnetic flux that in turn will tend to cancel the magnetic field generated by the generator circuit current coupled to the receptor circuit [1]. In this work, in order to simplify the modeling process, the second kind of grounding condition is considered.

Exposed sections of wire at the ends of the shield referred to as "pigtails" allow the fields to directly couple to the receptor wire and can significantly degrade the effectiveness of the shield in reducing

Table 1. Grouping criterion for the new simplification method.

	Near End	Far End
Group 1	$\|Z_N\| > Z_{cm}^c$	$\|Z_F\| > Z_{cm}^c$
Group 2	$\|Z_N\| > Z_{cm}^c$	$\|Z_F\| < Z_{cm}^c$
Group 3	$\|Z_N\| < Z_{cm}^c$	$\|Z_F\| > Z_{cm}^c$
Group 4	$\|Z_N\| < Z_{cm}^c$	$\|Z_F\| < Z_{cm}^c$

the crosstalk [17]. In this paper, we assume that the influence of the pigtail sections can be neglected considering that the pigtail sections all exist in the complete and reduced model. A braid will allow a certain amount of signal from the inside of the cable to leak through the surface transfer impedance [12]; however, little influence is on the simplified modeling for the reduced CCs and ignored in this work. Meanwhile, the following assumptions are made i) all conductors except the shield are considered as PEC, and the medium surrounding the culprit cable, victim cable, and the shield is assumed to be lossless, ii) the shield is uniform along the lines, which implies that the coupling mechanisms are independent of position along the line, and iii) only transverse electromagnetic (TEM) mode is propagated inside and outside the CCs.

2.2. Presentation of the Simplification Method

Step I: Grouping of Conductors

In this step, we will sort all the conductors of the complete cable bundle into different groups according to the grouping criterion shown in Table 1, in which, $|Z_{N(F)}|$ connected at both ends of the IC represents the near (far) end load impedance. Z_{cm}^c represents the common-mode (CM) characteristic impedance of the MCCB (denoted as superscript c) as Eq. (2). If the modulus of a load is very close to Z_{cm}^c, the conductor can be placed arbitrarily in one group or the other because this conductor will have insignificant influence on the group CM current due to the energy absorption in the load [13].

The determination of Z_{cm}^c requires the use of the modal theory [14] in order to obtain the characteristic of all the modes propagating along the cable. The diagonalization of the product of the per-unit-length (p.u.l.) matrices of the MTL provides the modal basis. For a single coaxial cable, when the shield is connected to the ground plane at

both ends, the characteristic impedance can be calculated as [1]

$$Z_c^c = \sqrt{\frac{l}{c}} = \sqrt{\frac{\frac{\mu_0}{2\pi}\ln(r^s/r^i)}{\frac{2\pi\epsilon_0\epsilon_r}{\ln(r^s/r^i)}}} = \sqrt{\frac{l^i - l^s}{c^{is}}}, \tag{1}$$

where l^i, l^s represent the p.u.l. inductance produced by IC (denoted as superscript i) and shield (denoted as superscript s), and r^i, r^s represent radii of the IC and shield. c^{is} represents the p.u.l. mutual capacitance between the IC and shield.

According to the modal analysis [14], the CM characteristic impedance of the MCCB can be written as follows, in which $L_{ij}^{is} = L_{ij}^{si}$

$$Z_{cm}^c = \frac{1}{n}\sqrt{\frac{\sum_{i=1}^{n}\sum_{j=1}^{n}(L_{ij}^{ii} - L_{ij}^{ss})}{\sum_{i=1}^{n}\sum_{j=1}^{n}C_{ij}^{is}}}. \tag{2}$$

Step II: Reduced Cable Bundle Matrices

1) General MTLN System of MCCB

According to the MTLN theory [1], for an N-CCs, the MTLN equations can be written in the following form:

$$\frac{\partial}{\partial z}\begin{bmatrix} V^i \\ V^s \end{bmatrix}_N = -\left[R + j\omega L\right]_{2N\times 2N} \cdot \begin{bmatrix} I^i \\ I^s \end{bmatrix}_N, \tag{3}$$

$$\frac{\partial}{\partial z}\begin{bmatrix} I^i \\ I^s \end{bmatrix}_N = -\left[G + j\omega C\right]_{2N\times 2N} \cdot \begin{bmatrix} V^i \\ V^s \end{bmatrix}_N, \tag{4}$$

where V^i, I^i, V^s and I^s represent the voltage and current flowing on the IC and shield, and R, L, G and C represent the p.u.l. parameters resistance, inductance, conductance and capacitance matrices of the IC and shield, respectively. $R^i = 0$ and $G = 0$ according to the above assumptions.

2) Determination of the p.u.l. Parameter Matrices of the RCB

This step is to determine the p.u.l. parameter matrices of the RCB model. Some approximations are made. For each group of conductors, we define a group-current $I_{gc}^{i(s)}$ and a group voltage $V_{gc}^{i(s)}$, respectively, and assume that the currents flow along each IC and shield belonging to the same group are identical. For example, the above assumptions

of a group i containing m CCs can be written as

$$I_{gci}^{i(s)} = I_1^{i(s)} + I_2^{i(s)} + \ldots + I_m^{i(s)}, \tag{5}$$

$$V_{gci}^{i(s)} = V_1^{i(s)} = V_2^{i(s)} = \ldots = V_m^{i(s)}, \tag{6}$$

$$I_k^{i(s)} = \frac{I_{gci}^{i(s)}}{m}. \tag{7}$$

In order to clearly show the derivation of the p.u.l. matrices of the RCB, we prefer to changing the index of the conductors belonging to the same group [14] as 1) the N_1 conductors of the first group have the index 1 to α, 2) the N_2 conductors of the second group have the index $\alpha+1$ to β, 3) the N_3 conductors of the third group have the index $\beta+1$ to γ and 4) the N_4 conductors of the fourth group have the index $\gamma+1$ to N.

In the MTL formalism, the inductance matrix links the currents and voltages on each conductor on an infinitesimal segment of length dz,

$$\frac{\partial}{\partial z}\begin{bmatrix} \ddot{V}_1^i \\ \ddot{V}_1^s \\ \vdots \\ \ddot{V}_k^i \\ \ddot{V}_k^s \\ \vdots \\ \ddot{V}_n^i \\ \ddot{V}_n^s \end{bmatrix} = -j\omega \begin{bmatrix} L_{11}^{ii} & L_{11}^{is} & \ldots & L_{1k}^{ii} & L_{1k}^{is} & \ldots & L_{1n}^{ii} & L_{1n}^{is} \\ & L_{11}^{ss} & \ldots & L_{1k}^{si} & L_{1k}^{ss} & \ldots & L_{1n}^{si} & L_{1n}^{ss} \\ & & \ddots & \vdots & \vdots & \vdots & \vdots & \vdots \\ & & & L_{kk}^{ii} & \ldots & \ldots & L_{kn}^{ii} & L_{kn}^{is} \\ & & & & L_{kk}^{ss} & \ldots & L_{kn}^{si} & L_{kn}^{ss} \\ & & & & & \ddots & \vdots & \vdots \\ & & & & & & L_{nn}^{ii} & L_{nn}^{is} \\ & & & & & & & L_{nn}^{ss} \end{bmatrix} \begin{bmatrix} Ic_1^i \\ Ic_1^s \\ \vdots \\ Ic_k^i \\ Ic_k^s \\ \vdots \\ Ic_n^i \\ Ic_n^s \end{bmatrix}, \tag{8}$$

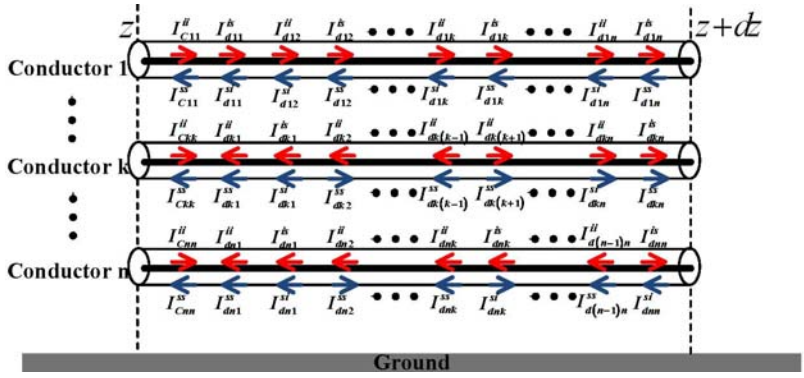

Figure 2. Decomposition of the CM and DM currents on a MCCB containing n CCs.

where the voltage $\ddot{V}_k^{i(s)}$ represents the inductive coupling voltage inducted by the kth IC (shield). The determination of the inductance matrix of the RCB requires two additional assumptions. To present and clearly justify these new assumptions, the currents flowing along the IC and shield of the n CCs are decomposed in Figure 2 into CM currents Ic_{ii}^{ii}, Ic_{ii}^{ss} and differential mode (DM) currents Id_{ij}^{ii}, Id_{ij}^{is}, Id_{ii}^{is} and Id_{ii}^{si}, where i and j represent conductor number. Thus, the currents I_1^i, I_k^i and I_n^i on IC and I_1^s, I_k^s and I_n^s on shield of the 1, k, and n CCs can be expressed as follows:

$$I_1^i = Ic_{11}^{ii} + \sum_{i=2}^{n}(Id_{1i}^{ii}) + \sum_{i=1}^{n}(Id_{1i}^{is}), \tag{9}$$

$$I_1^s = Ic_{11}^{ss} + \sum_{i=2}^{n}(Id_{1i}^{ss}) - Id_{11}^{si} + \sum_{i=2}^{n}(Id_{1i}^{si}), \tag{10}$$

$$I_k^i = Ic_{kk}^{ii} - \sum_{i=2}^{k-1}(Id_{ki}^{ii}) + \sum_{i=k+1}^{n}(Id_{ki}^{ii}) - \sum_{i=2}^{k-1}(Id_{ki}^{is}) + \sum_{i=k+1}^{n}(Id_{ki}^{is}), \tag{11}$$

$$I_k^s = Ic_{kk}^{ss} - \sum_{i=2}^{k-1}(Id_{ki}^{ss}) + \sum_{i=k+1}^{n}(Id_{ki}^{ss}) - \sum_{i=2}^{k-1}(Id_{ki}^{si}) + \sum_{i=k+1}^{n}(Id_{ki}^{si}), \tag{12}$$

$$I_n^i = Ic_{nn}^{ii} - \sum_{i=1}^{n-1}(Id_{ni}^{ii}) - \sum_{i=1}^{n-1}(Id_{ni}^{is}) + Id_{nn}^{is}, \tag{13}$$

$$I_n^s = Ic_{nn}^{ss} - \sum_{i=1}^{n-1}(Id_{ni}^{ss}) - \sum_{i=1}^{n}(Id_{ni}^{si}). \tag{14}$$

Taking Eqs. (9), (11), (13) into (8), the p.u.l. voltage of the kth IC can be written in the following form:

$$\begin{aligned}\frac{\partial \ddot{V}_k^i}{\partial z} &= -j\omega\left(L_{k1}^{ii}I_1^i + L_{k1}^{is}I_1^s + \ldots + L_{kk}^{ii}I_k^i + L_{kk}^{is}I_k^s + \ldots + L_{kn}^{ii}I_n^i + L_{kn}^{is}I_n^s\right) \\ &= -j\omega\left[\sum_{i=1}^{n}(L_{ki}^{ii}I_i^i) + \sum_{i=1}^{n}\left(L_{ki}^{is}I_i^s\right)\right],\end{aligned} \tag{15}$$

where

$$\begin{aligned}\sum_{i=1}^{n}L_{ki}^{ii}I_i^i = \sum_{i=1}^{n}L_{ki}^{ii}\left(Ic_{ii}^{ii}\right) + \Bigg[L_{k1}^{ii}\cdot\left(\sum_{i=2}^{n}Id_{1i}^{ii} + \sum_{i=2}^{k-1}Id_{ki}^{is}\right) \\ + \ldots + L_{kk}^{ii}\cdot\left(\sum_{i=2}^{k-1}Id_{ki}^{ii} + \sum_{i=k+1}^{n}Id_{ki}^{ii} - \sum_{i=2}^{k-1}Id_{ki}^{is} + \sum_{i=k+1}^{n}Id_{ki}^{is}\right)\end{aligned}$$

$$+\ldots+L_{kn}^{ii}\cdot\left(\sum_{i=1}^{n-1}Id_{ni}^{ii}-\sum_{i=2}^{n-1}Id_{ni}^{is}+Id_{nn}^{is}\right)\Bigg], \tag{16}$$

$$\begin{aligned}\sum_{i=1}^{n}L_{ki}^{is}I_i^s=&\sum_{i=1}^{n}L_{ki}^{is}(Ic_{ii}^{ss})+\Bigg[L_{k1}^{is}\cdot\left(\sum_{i=2}^{n}Id_{1i}^{ss}+\sum_{i=2}^{k-1}Id_{ki}^{is}\right)\\&+\ldots+L_{kk}^{is}\cdot\left(\sum_{i=2}^{k-1}Id_{ki}^{ii}+\sum_{i=k+1}^{n}Id_{ki}^{ii}-\sum_{i=2}^{k-1}Id_{ki}^{is}+\sum_{i=k+1}^{n}Id_{ki}^{is}\right)\\&+\ldots+L_{kn}^{ii}\cdot\left(\sum_{i=1}^{n-1}Id_{ni}^{ii}-\sum_{i=2}^{n-1}Id_{ni}^{is}+Id_{nn}^{is}\right)\Bigg].\end{aligned} \tag{17}$$

Consequently, the $\frac{\partial\ddot{V}_k^i}{\partial z}$ on an infinitesimal segment of length dz equals the sum of a term depending on the CM currents Ic_{ii}^{ii}, Ic_{ii}^{ss} and a term depending on DM currents Id_{ii}^{is}, Id_{ii}^{si} between conductor k and all the other conductors. The assumption made in the new equivalence technique also considers that the CM response is more critical than the DM response [13–15]. This assumption can be generalized with the following equation

$$\frac{\partial\ddot{V}_k^i}{\partial z}=-j\omega\left[\sum_{i=1}^{n}\left(L_{ki}^{ii}Ic_{ii}^{ii}\right)+\sum_{i=1}^{n}\left(L_{ki}^{is}Ic_{ii}^{ss}\right)\right]. \tag{18}$$

Similarly, for the shield system, the $\frac{\partial\ddot{V}_k^s}{\partial z}$ can be obtained as follows:

$$\frac{\partial\ddot{V}_k^s}{\partial z}=-j\omega\left[\sum_{i=1}^{n}\left(L_{ki}^{si}Ic_{ii}^{ii}\right)+\sum_{i=1}^{n}\left(L_{ki}^{ss}Ic_{ii}^{ss}\right)\right]. \tag{19}$$

The matrix linking the voltages on each conductor $\ddot{V}_i^i$ and $\ddot{V}_i^s$ to the CM current on each conductor can be written in the following form:

$$\frac{\partial}{\partial z}\begin{bmatrix}\ddot{V}_1^i\\ \ddot{V}_1^s\\ \vdots\\ \ddot{V}_k^i\\ \ddot{V}_k^s\\ \vdots\\ \ddot{V}_n^i\\ \ddot{V}_n^s\end{bmatrix}=-j\omega\begin{bmatrix}L_{11}^{ii} & L_{11}^{is} & \ldots & L_{1k}^{ii} & L_{1k}^{is} & \ldots & L_{1n}^{ii} & L_{1n}^{is}\\ & L_{11}^{ss} & \ldots & L_{1k}^{si} & L_{1k}^{ss} & \ldots & L_{1n}^{si} & L_{1n}^{ss}\\ & & \ddots & \vdots & \vdots & \vdots & \vdots & \vdots\\ & & & L_{kk}^{ii} & \ldots & \ldots & L_{kn}^{ii} & L_{kn}^{is}\\ & & & & L_{kk}^{ss} & \ldots & L_{kn}^{si} & L_{kn}^{ss}\\ & & & & & \ddots & \vdots & \vdots\\ & & & & & & L_{nn}^{ii} & L_{nn}^{is}\\ & & & & & & & L_{nn}^{ss}\end{bmatrix}\begin{bmatrix}Ic_{11}^{ii}\\ Ic_{11}^{ss}\\ \vdots\\ Ic_{kk}^{ii}\\ Ic_{kk}^{ss}\\ \vdots\\ Ic_{nn}^{ii}\\ Ic_{nn}^{ss}\end{bmatrix}. \tag{20}$$

So, the p.u.l. voltage of the IC and shield of the kth coaxial cable

can be rewritten as:

$$\frac{\partial \ddot{V}_k^i}{\partial z} = -j\omega\left[\sum_{j=1}^{\alpha}\left(L_{kj}^{ii}\cdot\frac{I_{gc1}^i}{N_1}\right)+\sum_{j=1}^{\alpha}\left(L_{kj}^{is}\cdot\frac{I_{gc1}^s}{N_1}\right)+\sum_{j=\alpha+1}^{\beta}\left(L_{kj}^{ii}\cdot\frac{I_{gc2}^i}{N_2}\right)\right.$$
$$+\sum_{j=\alpha+1}^{\beta}\left(L_{kj}^{is}\cdot\frac{I_{gc2}^s}{N_2}\right)+\sum_{j=\beta+1}^{\gamma}\left(L_{kj}^{ii}\cdot\frac{I_{gc3}^i}{N_3}\right)+\sum_{j=\beta+1}^{\gamma}\left(L_{kj}^{is}\cdot\frac{I_{gc3}^s}{N_3}\right)$$
$$\left.+\sum_{j=\gamma+1}^{N}\left(L_{kj}^{ii}\cdot\frac{I_{gc4}^i}{N_4}\right)+\sum_{j=\gamma+1}^{N}\left(L_{kj}^{is}\cdot\frac{I_{gc4}^s}{N_4}\right)\right], \tag{21}$$

$$\frac{\partial \ddot{V}_k^s}{\partial z} = -j\omega\left[\sum_{j=1}^{\alpha}\left(L_{kj}^{si}\cdot\frac{I_{gc1}^i}{N_1}\right)+\sum_{j=1}^{\alpha}\left(L_{kj}^{ss}\cdot\frac{I_{gc1}^s}{N_1}\right)+\sum_{j=\alpha+1}^{\beta}\left(L_{kj}^{si}\cdot\frac{I_{gc2}^i}{N_2}\right)\right.$$
$$+\sum_{j=\alpha+1}^{\beta}\left(L_{kj}^{ss}\cdot\frac{I_{gc2}^s}{N_2}\right)+\sum_{j=\beta+1}^{\gamma}\left(L_{kj}^{si}\cdot\frac{I_{gc3}^i}{N_3}\right)+\sum_{j=\beta+1}^{\gamma}\left(L_{kj}^{ss}\cdot\frac{I_{gc3}^s}{N_3}\right)$$
$$\left.+\sum_{j=\gamma+1}^{N}\left(L_{kj}^{si}\cdot\frac{I_{gc4}^i}{N_4}\right)+\sum_{j=\gamma+1}^{N}\left(L_{kj}^{ss}\cdot\frac{I_{gc4}^s}{N_4}\right)\right]. \tag{22}$$

Then, through modal analysis [14], we can obtain the $[L_{reduced}]$ matrix of the RCB, and the transmission line equation of the RCB can be rewritten in the following form:

$$\frac{\partial}{\partial z}\begin{bmatrix}\ddot{V}_{gci}^i\\ \ddot{V}_{gci}^s\end{bmatrix}_{8\times1} = -j\omega\ [L_{reduced}]_{8\times8}\cdot\begin{bmatrix}I_{gci}^i\\ I_{gci}^s\end{bmatrix}_{8\times1}. \tag{23}$$

Similarly, we can also obtain the $[R_{reduced}]$ and $[C_{reduced}]$ matrix of the RCB in the following form, in which $\dot{V}^{i(s)}$ represents the coupling voltage caused by p.u.l. resistance of the IC (shield).

$$\frac{\partial}{\partial z}\begin{bmatrix}\dot{V}_{gci}^i\\ \dot{V}_{gci}^s\end{bmatrix}_{8\times1} = -[R_{reduced}]_{8\times8}\cdot\begin{bmatrix}I_{gci}^i\\ I_{gci}^s\end{bmatrix}_{8\times1}, \tag{24}$$

$$\frac{\partial}{\partial z}\begin{bmatrix}I_{gci}^i\\ I_{gci}^s\end{bmatrix}_{8\times1} = -j\omega\ [C_{reduced}]_{8\times8}\cdot\begin{bmatrix}V_{gci}^i\\ V_{gci}^s\end{bmatrix}_{8\times1}. \tag{25}$$

Step III: Reduced Cable Bundle Cross-section Geometry

This step is to build the RCB model cross-section geometry. The operation is realized thanks to the knowledge of the $[L_{reduced}]$ and $[C_{reduced}]$ matrices. An optimization procedure made of six phases is necessary.

1) Phase 1: Calculate the height $h_i^{i(s)}$ above the ground reference of each RCB. The height $h_i^{i(s)}$ of each RCB corresponds to the average height of all the IC and shield of the CCs belonging to the ith group, and it should be noticed $h_i^i = h_i^s$ in a coaxial cable that we only need to calculate h_i^i or h_i^s.

2) Phase 2: Calculate the radius r^s of the shield of each RCB according to the analytical formula as follows [1]

$$r^s = \frac{2 \cdot h_i}{\exp\left(\dfrac{2\pi \cdot L^s_{ii\_reduced}}{\mu_0}\right)}. \tag{26}$$

3) Phase 3: Calculate the radius r^i of the IC of each equivalent coaxial cable according to the analytical formula as follows [1]

$$r^i = \frac{2 \cdot h_i}{\exp\left(\dfrac{2\pi \cdot L^i_{ii\_reduced}}{\mu_0}\right)}. \tag{27}$$

4) Phase 4: Calculate the distances d_{ij} between all RCB according to the following formula. Considering that $L^i_{ij} = L^s_{ij} = L^{is}_{ij}$ here, we arbitrarily take L^i_{ij} into the formula [1].

$$d_{ij} = \sqrt{\frac{4h_i h_j}{\exp\left(\dfrac{4\pi \cdot L^i_{ij\_reduced}}{\mu_0}\right) - 1}}. \tag{28}$$

5) Phase 5: Determine the thickness of the dielectric coating T_{PE} surrounding the IC and T_{PVC} surrounding the shield of each RCB while avoiding dielectric coating overlapping.

6) Phase 6: Adjust h_i, r^i, r^s, d_{ij} determined by the above procedures using a dichotomic optimization [13] realized with exact electrostatic calculations in error range. Calculate the relative permittivity ε_r of each RCB dielectric coating according to the $[C_{reduced}]$ matrix using an electrostatic calculation.

Figure 3 illustrates the six-phase procedure used to build the cross-section geometry of a RCB made of three groups.

Step IV: Reduced Cable Bundle Equivalent Termination Loads

This step is the same as in [13, 14] and omitted here without affecting the integrity of this paper.

Step V: Application of the MTLN Methods to EM Crosstalk of the Cable Bundle Model

Once the RCB model is obtained, we can apply the MTLN method in the prediction of EM crosstalk problems.

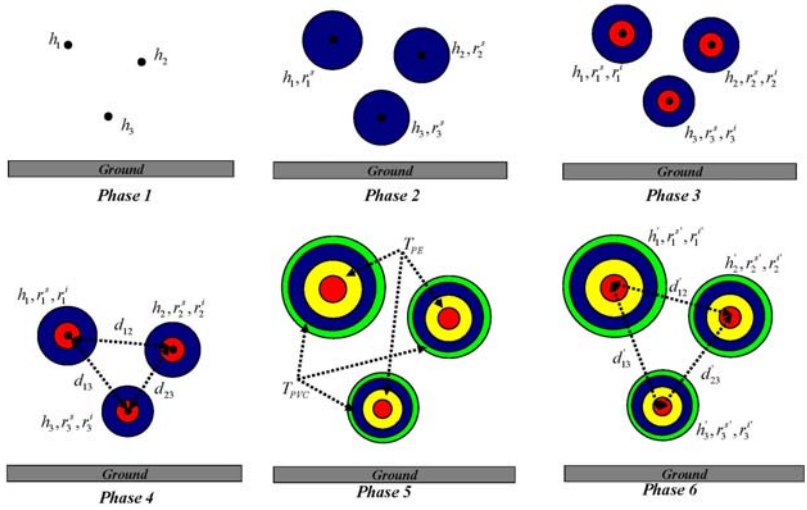

Figure 3. Six-phase procedure for building the cross-section geometry of a RCB containing three equivalent CCs.

3. VALIDATIONS OF THE SIMPLIFICATION METHOD FOR CROSSTALK PREDICTION THROUGH NUMERICAL SIMULATIONS

As a numerical validation of the simplification method, a 9-conductor point-to-point connected cable bundle, 0.5 m long, set above an infinite PEC ground plane shown in Figure 4(a) is investigated, in which all conductors are braided CCs of the RG58 model. The corresponding parameters are listed in Table 3, and both ends of the shield except Cable 1 are connected to the ground plane. The near end of the IC of Cable 1 (culprit cable) is excited with a periodic trapezoidal pulse voltage source whose amplitude equals 100 volts, rising edge $\tau_r = 2$ nanosecond (ns), falling edge $\tau_f = 2$ ns, pulse width $\tau = 62$ ns and cycle time $T_t = 200$ ns, and Cable 2 serves as the victim cable. The p.u.l. inductance $[L]$ (in nanohenry/meter) and capacitance $[C]$ matrices (in picoferad/meter) of Cables 3∼9 in the cable bundle are listed in (29) and (30), which can be used to calculate the CM characteristic impedance Z^c_{cm} that equals 41 Ω.

Meanwhile, the near and far end loads of Cables 1∼9 are listed in Table 2. According to the grouping rule in Section 2, the conductors of cable 3∼9 can be sorted into three groups (Group 1: Cables 3∼5,

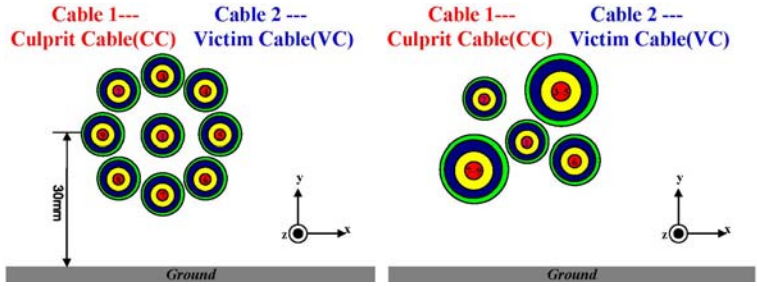

Figure 4. Cross-section geometry. (a) The complete model. (b) The reduced model.

Group 2: Cable 6, Group 3: Cables 7∼9) shown in Figure 4(b).

$$[L]=\begin{bmatrix}
866 & 637 & 478 & 478 & 397 & 397 & 352 & 352 & 339 & 339 & 352 & 352 & 397 & 397 \\
 & 637 & 478 & 478 & 397 & 397 & 325 & 352 & 339 & 339 & 352 & 352 & 397 & 397 \\
 & & 860 & 631 & 464 & 464 & 381 & 381 & 344 & 344 & 338 & 338 & 360 & 360 \\
 & & & 631 & 464 & 464 & 381 & 381 & 344 & 344 & 338 & 338 & 360 & 360 \\
 & & & & 840 & 611 & 444 & 444 & 368 & 368 & 339 & 339 & 342 & 342 \\
 & & & & & 611 & 444 & 444 & 368 & 368 & 339 & 339 & 342 & 342 \\
 & & & & & & 818 & 590 & 428 & 428 & 361 & 361 & 340 & 340 \\
 & & & & & & & 590 & 428 & 428 & 361 & 361 & 340 & 340 \\
 & & & & & & & & 808 & 580 & 428 & 428 & 368 & 368 \\
 & & & & & & & & & 580 & 428 & 428 & 368 & 368 \\
 & & & & & & & & & & 818 & 590 & 444 & 444 \\
 & & & & & & & & & & & 590 & 444 & 444 \\
 & & & & & & & & & & & & 840 & 611 \\
 & & & & & & & & & & & & & 611
\end{bmatrix}_{14\times14}, \tag{29}$$

$$[C]=\begin{bmatrix}
111.9 & -111.9 & 0 & 0 & 0 & 0 & 0 & 0 & 0 & 0 & 0 \\
 & 183.9 & 0 & -40.1 & 0 & -2.7 & 0 & -1.9 & 0 & -2.0 & 0 \\
 & & 111.9 & -111.9 & 0 & 0 & 0 & 0 & 0 & 0 & 0 \\
 & & & 200.7 & 0 & -39.2 & 0 & -1.8 & 0 & -1.3 & 0 \\
 & & & & 111.9 & -111.9 & 0 & 0 & 0 & 0 & 0 \\
 & & & & & 201.4 & 0 & -39.0 & 0 & -1.9 & 0 \\
 & & & & & & 111.9 & -111.9 & 0 & 0 & 0 \\
 & & & & & & & 201.1 & 0 & -38.9 & 0 \\
 & & & & & & & & 111.9 & -111.9 & 0 \\
 & & & & & & & & & 201.8 & 0 \\
 & & & & & & & & & & 111.9
\end{bmatrix}$$

$$\begin{bmatrix}
0 & 0 & 0 \\
-2.1 & 0 & -19.4 \\
0 & 0 & 0 \\
-1.2 & 0 & -2.2 \\
0 & 0 & 0 \\
-1.3 & 0 & -2.0 \\
0 & 0 & 0 \\
-1.6 & 0 & -1.8 \\
0 & 0 & 0 \\
-38.9 & 0 & -2.4 \\
-111.9 & 0 & 0 \\
201.1 & 0 & -39.8 \\
 & 111.9 & -111.9 \\
 & & 184.1
\end{bmatrix}_{14\times14}. \tag{30}$$

After some simple calculations, the p.u.l. inductance $[L]$ (in nanohenry/meter) and capacitance $[C]$ (in picoferad/meter) of the

Table 2. Termination loads of the 9-conductor complete cable bundle (unit: Ω).

Conductor	1	2	3	4	5	6	7	8	9
Near End	50	100	20	15	30	20	5 k	2 k	1 k
Far End	50	200	10	18	25	800	2 k	1 k	2.5 k

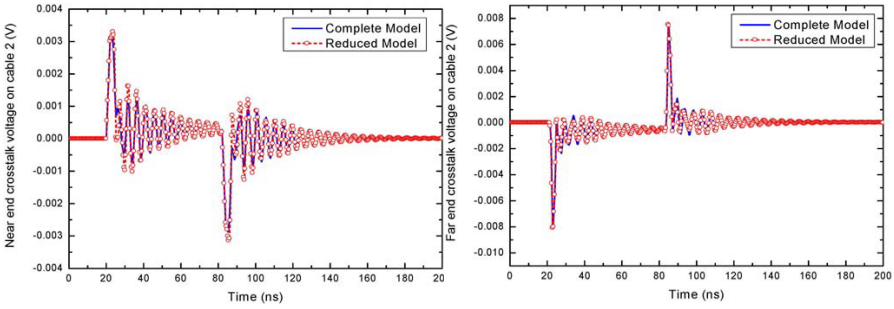

(a) (b)

Figure 5. Comparison of the crosstalk voltage in the time domain on Cable 2 between the complete and reduced cable bundle models. (a) Near end. (b) Far end.

RCB model are listed in (31) and (32).

$$[L_{reduced}] = \begin{bmatrix} 583 & 506 & 392 & 392 & 353 & 353 \\ & 506 & 392 & 392 & 353 & 353 \\ & & 818 & 590 & 376 & 376 \\ & & & 590 & 376 & 376 \\ & & & & 550 & 473 \\ & & & & & 473 \end{bmatrix}_{6\times6}, \tag{31}$$

$$[C_{reduced}] = \begin{bmatrix} 335.7 & -335.7 & 0 & 0 & 0 & 0 \\ & 422.0 & 0 & -42.7 & 0 & -33.5 \\ & & 111.9 & -111.9 & 0 & 0 \\ & & & 201.1 & 0 & -42.2 \\ & & & & 335.7 & -335.7 \\ & & & & & 424.8 \end{bmatrix}_{6\times6}. \tag{32}$$

After applying the six-procedure described in Section 2, we obtain the cross-section geometry of the RCB model composed of five equivalent conductors shown in Figure 4(b). The equivalent termination loads connected to each end of all IC and the corresponding parameters of the RCB can be easily obtained and are listed in Table 3.

The near and far ends crosstalk voltage in the time domain and frequency domain (0–500 MHz) on Cable 2 can finally be obtained by applying the MTLN to the complete and reduced models shown in Figure 5 and Figure 6, respectively. The good agreement of both curves of Figures 5 and 6 validates the EM crosstalk problem for both cable bundle models and this new simplification method.

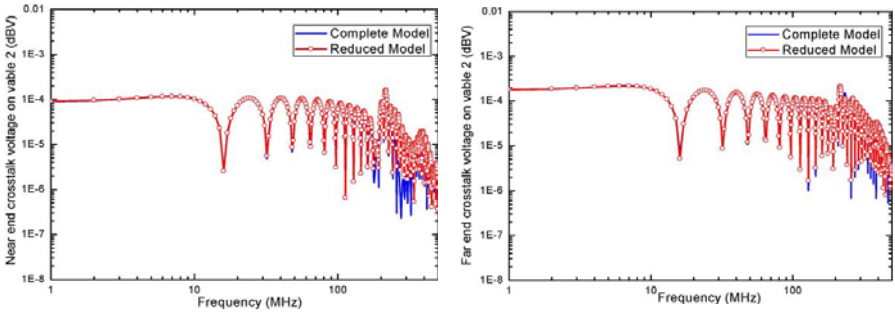

Figure 6. Comparison of the crosstalk voltage in the time domain on Cable 2 between the complete and reduced cable bundle models. (a) Near end. (b) Far end.

Table 3. Termination loads (unit: Ω) and some parameters of the RCB (unit: mm).

Conductor	1	2	3∼5	6	7∼9
Near End	50	100	6.7	20	588.3
Far End	50	200	5.1	800	526.3
Radius of IC	0.47	0.47	3.7	0.85	3.4
Insulator Inside of PE	1.005	1.005	1.005	1.005	1.005
Radius of Braided Shield	1.8	1.8	5.4	2.7	4.9
Insulator Outside of PVC	0.5	0.5	0.5	0.5	0.5

4. CONCLUSIONS

This paper details the theoretical basis of the new simplification method for modeling crosstalk of the MCCB. The analysis of the voltages and currents in CCs allows us to create a RCB model containing a limited number of equivalent conductors. When applied to a cable harness case, a modified five-step procedure is established to define the electrical and geometrical characteristics of the RCB model. The good agreement of the numerical simulation results between the complete and reduced cable bundle models validates the efficiency and advantages of the proposed method.

The main purpose of the new simplification method is to reduce the complexity and computation time, and the total computation time is reduced by a factor of 3.9 (Complete model costs 39 seconds,

Reduced model costs 10 seconds) after equivalence of the complete model by using the method of MTLN, which have been performed on a 2.3-GHz processor and a 2.0-GB RAM memory computer. All these results fully demonstrate that the method can significantly reduce the prediction time and memory requirement.

ACKNOWLEDGMENT

This work was supported by the National Natural Science Foundation of China for Young Scholars under Grant No. 61102033, the Fundamental Research Funds for the Central Universities under Grant NS2012096, the Foundation of State Key Laboratory of Millimeter Waves, Southeast University, P. R. China under Grant No. K201302 and the Aeronautical Science Foundation of China under grant No. 20128052063.

REFERENCES

1. Paul, C. R., *Analysis of Multiconductor Transmission Lines,* Wiley-Interscience, New York, 1994.
2. Sali, S., F. A. Benson, and J. E. Sitch, "Coupling between multi-coaxial cable systems. Part I: General considerations and efficient numerical method for crosstalk," *IEE Proc.,* Vol. 129, No. 3, 162–166, May 1982.
3. Wang, J., W.-Y. Yin, J.-P. Fang, and Q.-F. Liu, "Transient responses of coaxial cables in an electrically large cabin with slots and windows illuminated by an electromagnetic pulse," *Progress In Electromagnetics Research,* Vol. 106, 1–16, 2010.
4. Koo, S. K., H. S. Lee, and Y. B. Park, "Crosstalk reduction effect of asymmetric stub loaded lines," *Journal of Electromagnetic Waves and Applications,* Vol. 25, Nos. 8–9, 1156–1167, 2011.
5. Lin, D.-B., F.-N. Wu, W. S. Liu, C. K. Wang, and H.-Y. Shih, "Crosstalk and discontinuities reduction on multi-module memory bus by particle swarm optimization," *Progress In Electromagnetics Research,* Vol. 121, 53–74, 2011.
6. Shamaileh, K. A. A., A. M. Qaroot, and N. I. Dib, "Non-uniform transmission line transformers and their application in the design of compact multi-band Bagley power dividers with harmonics suppression," *Progress In Electromagnetics Research*, Vol. 113, 269–284, 2011.
7. Wu, Y. and Y. Liu, "An unequal coupled-line Wilkinson

power divider for arbitrary terminated impedances," *Progress In Electromagnetics Research*, Vol. 117, 181–194, 2011.

8. Deng, P.-H., J.-H. Guo, and W.-C. Kuo, "New wilkinson power dividers based on compact stepped-impedance transmission lines and shunt open stubs," *Progress In Electromagnetics Research*, Vol. 123, 407–426, 2012.
9. Liu, Y., L. Tong, W. Zhu, Y. Tian, and B. Gao, "Impedance measurements of nonuniform transmission lines in time domain using an improved recursive multiple reflection computation method," *Progress In Electromagnetics Research*, Vol. 117, 149–164, 2011.
10. Sali, S., "Transfer impedance of braided coaxial cables at radio and microwave frequencies," M. Eng. Thesis, University of Sheffield, UK, 1979.
11. Benson, F. A., P. A. Cudd, and J. M. Tealby, "Leakage from coaxial cables," *IEE Proc.,* Vol. 139, No. 6, 285–303, Nov. 1992.
12. Tealby, J. M., P. A. Cudd, and F. A. Benson, "Coupling between jacketed braided coaxial cables," *IEE Proc.,* Vol. 134, No. 10, 793–798, Dec. 1987.
13. Andrieu, G., L. Koné, F. Bocquet, B. Démoulin, and J. P. Parmantier, "Multiconductor reduction technique for modeling common-mode currents on cable bundles at high frequency for automotive applications," *IEEE Trans. Electromagn. Compat.,* Vol. 50, No. 1, 175–184, Feb. 2008.
14. Andrieu, G., X. Bunlon, L. Koné, J. P. Parmantier, B. Démoulin, and A. Reineix, "The 'equivalent cable bundle method': An efficient multiconductor reduction technique to model industrial cable networks," *New Trends and Developments in Automotive System Engineering*, InTech, Jan. 2011.
15. Li, Z., L. L. Liu, and C. Q. Gu, "Generalized equivalent cable bundle method for modeling EMC issues of complex cable bundles terminated in arbitrary loads," *Progress In Electromagnetic Research,* Vol. 123, 13–30, 2012.
16. Schetelig, B., J. Keghie, R. Kanyou Nana, L.-O. Fichte, S. Potthast, and S. Dickmann, "Simplified modeling of EM field coupling to complex cable bundles," *Adv. Radio Sci.*, Vol. 8, 211–217, 2010.
17. Paul, C. R., "Effect of pigtails on crosstalk to braided-shield cables," *IEEE Trans. Electromagn. Compat.,* Vol. 22, No. 3, Aug. 1980.